THE SOCIOECONOMIC DETERMINANTS OF PANDEMICS: A SPATIAL METHODOLOGICAL APPROACH WITH EVIDENCE FROM COVID-19 IN NICE, FRANCE

Documents de travail GREDEG
GREDEG Working Papers Series

Laurent Bailly
Rania Belgaied
Thomas Jobert
Benjamin Montmartin

GREDEG WP No. 2025-04
https://ideas.repec.org/s/gre/wpaper.html

The Socioeconomic Determinants of Pandemics: A Spatial Methodological Approach with Evidence from COVID-19 in Nice, France

Université Côte d'Azur, CNRS, GREDEG, France

Authors:

Bailly Laurent (Hospital Practitioner Public Health Department at CHU Nice)

Belgaied Rania (Ph.D Student)

Jobert Thomas (University Professor of Economic Sciences)

Montmartin Benjamin (Associate Professor of Econometrics and Data Science)

Abstract:

During the period from January 4 to February 14, 2021 the spread of the COVID epidemic peaked in the city of Nice, with a worrying number of infected cases. The spatial dynamics of the pandemic revealed explicit geographical patterns. This article focuses on analyzing the spatial pattern of virus spread and assessing the geographical factors influencing this distribution. Thus, in this article, spatial modeling was carried out to examine geographical disparities in terms of distribution, incidence and prevalence of the virus, while taking socio-economic factors into account. A multiple linear regression model was used to identify the key socio-economic variables affecting the spread of COVID-19 in Nice. Global and local spatial autocorrelation was measured using Moran and LISA indices, followed by spatial autocorrelation analysis of the residuals. Similarly, we used a global regression model and local models (the Geographically Weighted Regression (GWR) model and the Multiscale Geographically Weighted Regression (MGWR) model), to assess the influence of socio-economic factors that vary on a global and local scale, in order to adopt the most appropriate model explaining the spread of the disease. The results confirm that covid-19 is strongly spatially correlated, and that spatial analysis is an essential step in implementing effective preventive measures. The various global and local models identified four significant variables with regard to vulnerability to COVID disease in Nice. Our results reveal a marked geographical polarization, with affluent areas in the southeast contrasting sharply with disadvantaged neighborhoods in the northwest. Neighborhoods with low LHDI, low levels of education, social housing and immigrant populations. These latter factors all point to worrying values. On the other hand, people who use public transport are significantly negatively correlated with contamination by the virus. These results underline the importance of geographically predicting COVID-19 distribution patterns to guide targeted interventions and health policies in Nice. Understanding these spatial patterns using models such as MGWR can help guide public health interventions and inform future health policies, particularly in the context of pandemics.

Key words: COVID-19, Spatial analysis, Spatial autocorrelation, Public health, Geographic Information System (GIS)

I- Introduction

The history of pandemics, from the Black Death in the 14th century to the Spanish flu of 1918 and the HIV/AIDS epidemic, shows that health crises are neither exceptional nor one-off. Numerous studies have shown that the emergence of new pandemics is inevitable[1–3], not least because of increased interactions between humans and the environment in an increasingly globalized world. These conditions favor the transmission of new pathogens on a global scale.

The methodology developed in this study can be applied to the analysis of many pandemics, whether past, present or future. Nevertheless, we have chosen to focus on the COVID-19 pandemic. There are two main reasons for this choice: its recent nature, which makes it particularly relevant, and the availability of reliable, up-to-date data to deepen our understanding of the socio-economic and spatial dynamics underlying its spread.

While pandemics have been widely studied from epidemiological or socio-economic angles, few studies have taken advantage of small-scale approaches, such as the one proposed here, at the IRIS level. This statistical unit, which divides French communes into homogeneous territories, reveals local disparities that are often masked by analyses on larger scales. By choosing to focus on the city of Nice, this study provides an original perspective on the socio-economic determinants influencing the spatial distribution of COVID-19 incidence, while highlighting the importance of the spatial scale in the analysis of health crises.

"Covid is not an equal opportunity Killer". This observation by J. Stiglitz is true in terms of both mortality rates[4–6] and incidence rates[7,8]. At the beginning of the pandemic, research focused on the epidemiological, clinical[8,9], environmental[10], demographic[11] and ecological characteristics of infected patients. However, as the pandemic evolved, other potential determinants, such as ethnicity or socio-economic factors, also appeared to play a significant role in explaining the spread of COVID-19[12–14]. Philip Schellekens and Diego Sourrouille[4] described COVID-19 as a missile aimed at the most vulnerable in society. Shahbazi and Khazaj[5], using the Human Development Index (HDI) as an indicator of the incidence and mortality rate of COVID-19, found that developed countries were the most affected. Similarly, Josephine Etowa, Ilene Hyman et al[15] show that the risk and burden of COVID infection are not evenly distributed between population subgroups. Claire Bambra , Ryan Riordan et al[16] explained the emergence of these inequalities through a syndemic approach to COVID-19, in view of the synergistic interaction between the incidence rate and the socio-environmental and socio-economic factors that foster such interaction and aggravate the situation of the COVID-19 health crisis. Hence, socio-economic deprivation is a key driver of COVID-19 virus incidence[17].

Since the appearance of the first COVID-19 infected case, several statistical models and methods published in recent years have resurfaced[18], some of which emphazie the prevalence of clusters in regions. Clusters represent groups of individuals burdened with the infection, where the highest number of infected cases are concentrated. Thus, a geolocalized study that considers spatial variation in incidence rates is essential.

The importance given to spatial analysis, considering location, spatial interaction, spatial structure and spatial processes is central to research in various fields, notably epidemiology, econometrics and environmental science. For example, in the field of economics, Patel et al[19] pointed out that during the pandemic period, the risk of exposure to coronavirus and of developing severe forms of the disease varies considerably according to housing overcrowding, working conditions, living or housing conditions, education level and income[20]. Thus, it is necessary to consider contextual elements in the analysis of a health-related issue at multiple levels. First, the structure of families within the same household, including overcrowding, foreign-born families, and immigrants[21]. Second, poverty[22] and the quality of the healthcare system also help explain differences between regions[23]. Demography is also a factor in spatial differentiation in health[24], whether national or regional[25]. Education level and the organization of the healthcare system also plays a role as a socio-economic approach to the geographical scale of COVID.

The aim of this study is to determine the link between the incidence of COVID-19 disease in the 144 districts of the city of Nice and their socio-economic characteristics, while considering spatial interactions between neighborhoods.

II- Method

According to the 2019 census[26], Nice has a population of 341,003 people spread over an area of 71.92 km², giving a density of 4741 inhabitants per km². INSEE statistics[27] show that the commune of Nice has a poverty rate of over 30% among tenant households as well as an unemployment rate of over 25% among young people aged 15 to 24. The study period runs from January 4 to February 14, 2021. The Nice metropolitan area recorded an average incidence rate of 463.5 cases per 100,000 inhabitants, above the alert threshold of 400 cases per 100,000[28] set by the health authorities. In all, 10,078 cases of COVID-19 were included in the study.

Our database is the result of a fusion of epidemiological, socio-economic, socio-demographic and socio-environmental data. Epidemiological data on the incidence rate of COVID-19 were provided by the "Système National d'Information sur le dépistage de la COVID-19" (SIDEP)[29] and concern residents of the city of Nice with a first positive screening test. Only sporadic cases were counted, excluding people in institutions for dependent elderly people. The COVID-19 incidence rate was used as a health indicator to assess the COVID epidemic, based on data published by the "Santé Publique France (SPF)" health agency. This agency is responsible for implementing a national health surveillance and alert system, and provides the French Ministry of Health with all the indicators needed to monitor the epidemic on a daily basis. The rest of the variables were obtained from databases of the French National Institute for Statistics and Economic Studies (INSEE)[26]. We selected 37 variables divided into 6 categories: "income/inequality, housing conditions, population density, contamination through work, understanding of health rules and cultural factors, and contamination through the school environment".

We selected five socio-economic variables, presented in Figure 1, based on a review of the literature and all available data, and using the LASSO method to select the variables with the best AIC. In addition to the LASSO method, we performed multiple linear regression on the variables using the OLS estimation method, which enabled a significant selection of variables. This minimized the potential problem of multicollinearity, thus avoiding any problems resulting from over-fitting. These five variables are the localized human development index (LHDI)[4–6,15], the proportion of the population living in low-income housing[4,7,10,30,31], the proportion of people using public transport[31–33], the proportion of the immigrant population[17,30,31,34–36], and the proportion of people aged between 18 and 24 who have attended school[11,33,37].

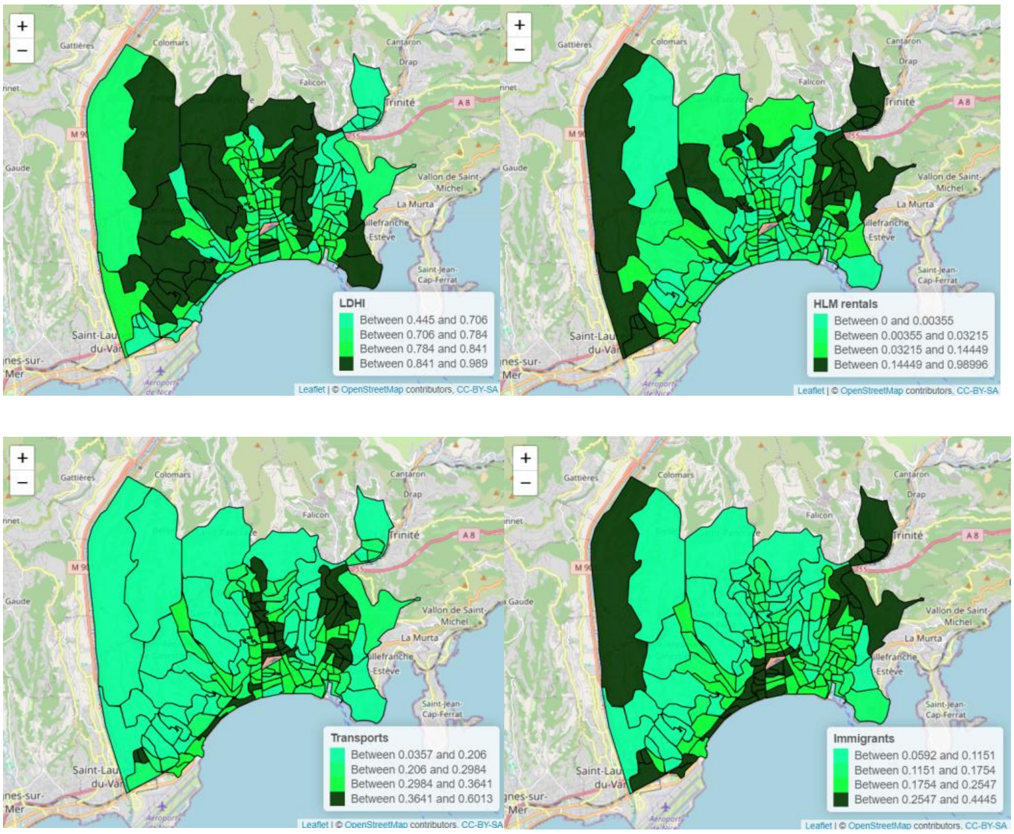

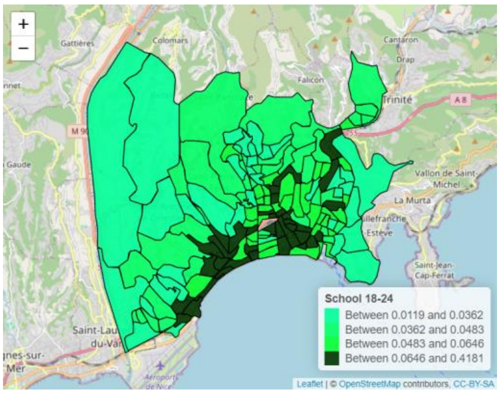

Figure 1 Cartographic representation of independent variables

We adopt an exploratory approach in two main phases. The first phase involves detecting the presence of spatial dependence[38] in the data using spatial autocorrelation. The second phase aims to explore nonlinear relationships between several socio-economic factors and incidence rates by applying GWR and MGWR regression models.

Developed from 1950 by Patrick Moran[39], spatial autocorrelation provides information on the spatial distribution of their study variables. This concept identifies significant groupings, or clusters, in space. This method highlights a relationship between neighbors that is more marked than the relationship with the rest of the IRIS studied. Thus, spatial autocorrelation is the correlation of a variable with itself, when observations are considered with a spatial offset[38]. The type of location used in this article is surface-based, since the observations are IRIS-based.

To quantify spatial autocorrelation, the Moran index was applied[40]. This index, which varies between [-1, +1], assesses the direction and intensity of spatial correlation. A positive value indicates a positive spatial correlation, while a negative value indicates a negative correlation[41]. The higher the index value, the stronger the spatial correlation[37]. Conversely, an index close to 0 indicates the absence of autocorrelation, suggesting a random distribution of observations.

The Moran's I formula is as follows:

$$\text{Moran's I } = \frac{\sum_i \sum_j w_i (z_i - \bar{z})(z_j - \bar{z})}{\sum_i (z_i - \bar{z})^2}$$

Where: z_i = value of the variable at point i and mean $\bar{z}$, i = individual, j = neighbors of individuals i, w_i= weighted matrix (neighborhood matrix).

Spatial weighted matrices are essential for capturing the interdependence between regions through their relative positions. There are 3 types of weighted matrix[40] with dimensions (n*n), where n is the number of IRIS. The distance matrix (Two IRIS are considered neighbors if they are situated within the defined neighborhood distance. The default distance is the shortest distance where each IRIS has at least one additional neighbor), the contiguity matrix (Two regions i and j are contiguous of order k if k is the minimum number of boundaries to cross to get from i to j.) and the neighborhood matrix (All IRIS have the same fixed number of neighbors).

Spatial autocorrelation can have several sources. It may come from spatially autocorrelated omitted variables, or from measurement errors: the effect not captured by the explanatory variables can appear in the errors in the form of spatial autocorrelation[38]. This will then be considered as a tool for diagnosing spatial dependence.

Residual spatial autocorrelation serves as an essential diagnostic for the correct specification of models. It can therefore be used to verify the existence of spatial dependence between residuals. Significant residual autocorrelation often indicates that important explanatory variables have been omitted or misspecified[41]. Therefore, by calculating the global Moran index for the regression residuals, we can detect these errors and adjust the model accordingly, ensuring a more accurate representation of the underlying spatial dynamics. Not using residuals leads to three major statistical problems in modelling: underestimation of standard errors, bias in parameter estimates, and model specification errors[42].

To this end, the Global Moran Index will be calculated in relation to the residuals of the regression estimated by the OLS (Ordinary Least Squares) model with the weight matrix. In this case, it takes the following matrix form:

$$I = \frac{N}{S_0}\left(\frac{\widetilde{\varepsilon'} W \tilde{\varepsilon}}{\widetilde{\varepsilon'}\tilde{\varepsilon}}\right)$$

Where: $\tilde{\varepsilon} = y - X\tilde{\beta}$ *is the vector of residuals from the OLS regression and* S_0 *a standardization factor equal to the sum of all elements of* W *(weighting matrix / neighborhood matrix).*

Although global indices of spatial autocorrelation, such as the Moran index, provide an overview of the spatial structure of the COVID-19 distribution, they can lack precision when it comes to highly localized phenomena[43]. The Local Indicator of Spatial Association (LISA) was applied to assess the local level of spatial autocorrelation or spatial data dependence and to detect the emergence of possible and potential clusters based on COVID-19 incidence rates in the 144 IRIS of the city of Nice. In other words, local associations between IRIS in proximity to each other are sought[44] The formula for Moran's local index is as follows:

$$I_i = x_i \sum_j w_{ij} x_j$$

Where x_i and x_j represent COVID incidence rates in IRIS i and j respectively, w_{ij} spatial weighting matrix.

The Local Moran Index (LISA) divides neighboring IRIS into four categories (High-High: Cluster-an area with a high incidence rate surrounded by neighbors with a high number of cases, High-Low: Area with a high incidence rate surrounded by neighbors with a low number of sick cases, Low-Low: Cluster-an area with a low incidence rate surrounded by a low-value area and finally Low-High: Area with a low incidence rate surrounded by a high-value area).

We used three different global and local spatial regression models to explain the relationship between our socio-economic variables and the COVID incidence rate. These include a global ordinary least squares (OLS) regression model and two local regression models: the local GWR model (the geographically weighted regression) and the multiscale GWR (MGWR).

Estimated using the OLS method, the model assumes that changes in space are universal. It is based on two major assumptions: firstly, observations are independent and constant within the study area, and secondly, there is no correlation between the error terms[30,45].

In this study, exploratory analyses revealed polarization and spatial heterogeneity in the distribution of COVID-19, justifying the use of statistical tools sensitive to intra-urban variations. In this context, Geographically Weighted Regression (GWR) and Multiscale Geographically Weighted Regression (MGWR) were applied[46,47]. Lagrange multiplier and robustness tests applied to the data did not reveal any significance. Unlike global models, the regression coefficients in the GWR model are not fixed, but vary according to the geographical coordinates of observations i in the Nice city. As a result, local regression parameter estimates are obtained at each observation point[48]. Thus, the coefficients of the explanatory parameters form continuous surfaces that are estimated at certain points in space[49].

$$y_i = \beta_0(u_i, v_i) + \sum_{k=1}^{p} \beta_k(u_i, v_i) x_{ik} + \epsilon_i$$

With y_i the dependent variable (COVID incidence rate), (μ_i, v_i)) vector form of coordinates x,y, Xi_k value of the kth explanatory parameter, ε_i random residuals.

The GWR model uses a single optimal bandwidth for all explanatory variables, which assumes that all factors affect the COVID-19 rate on the same spatial scale. In this study, a Gaussian kernel was used to weight observations according to their spatial proximity[50]. This choice progressively reduces the influence of observations as distance increases, giving more weight to nearby observations[49]. Model estimation is based on a matrix of weights W(i) whose values decrease as a function of the distance separating units i and j.

$$w(d_{ij}) = \exp\left(-\frac{1}{2}\left(\frac{d_{ij}}{b}\right)^2\right) \text{ if } d_{ij} < 0, 0 \text{ if not.}$$

The bandwidth b is estimated using a cross-validation approach, with the aim of minimizing the mean-square error MSE

$$MSE = \sum_{i=1}^{n} \left(y_i - \widehat{y_{i\neq\iota}}(b)\right)^2$$

The Gaussian kernel function used to weight the observations is essential for determining the spatial extent of the influence of neighboring observations. The coefficients β are obtained by minimizing the sum of the weighted squares:

$$\sum_{j=1}^{n} w_j(i)\left(y_j - \beta_0(u_i, v_i) - \sum_{k=1}^{p} \beta_k(u_i, v_i)x_{jk}\right)^2$$

With the weighted least squares estimator given by[49]:

$$\hat{\beta}(u_i, v_i) = (X^T W(u_i, v_i)X)^{-1} X^T W(u_i, v_i)Y$$

The choice of a single bandwidth can be penalizing, particularly when the explanatory variables influence the dependent variable at different spatial scales. This limitation can reduce the reliability of statistical inferences and bias results[48,51].

To counter these problems, Fotheringham and al[52] developed the MGWR model[53,54]. MGWR regression is an extension of GWR that allows the use of different optimal bandwidths specific to each explanatory variable, since it eliminates the assumption that there are variations within the same scale[53]. This multiscalar approach makes it possible to model spatial relationships more accurately, recognizing that each factor can influence COVID-19 levels on a different spatial scale. Allowing an optimal number of neighbors to be considered for each parameter estimate, which favors predictions of explanatory variables[55]. It is defined as[52]:

$$y_i = \beta_0(u_i, v_i) + \sum_{k=1}^{p} \beta_k(u_i, v_i, b_k)x_{ik} + \epsilon_i$$

With b_k non-fixed bandwidth specific to variable k

Local models were estimated using MGWR software version 2.2: Spatial Analysis Research Center (SPARC), Tempe,USA), developed by Fotheringham et al. (2017)[52]. Output and mapping were produced using Rstudio.

III- Results

Overall, each map (Figure1) shows a certain form of geographical polarization in Nice, with clear divisions in the distribution of socio-economic variables. Polarization is particularly marked for the LHDI, where there is a noticeable polarization between the center/southeast and the northwest of the city, where favored neighborhoods (center/southeast) contrast sharply with less favored areas (northwest). It is also strongly marked in the proportion of low-income housing, where the polarization is strong between the west (concentration of low-income housing) and the center-east (very few low-income housing). This reflects a concentration of social housing in specific areas, which could indicate residential segregation - some areas are clearly more favored or more concentrated in social housing than others. These polarities could reflect social, economic and service access inequalities.

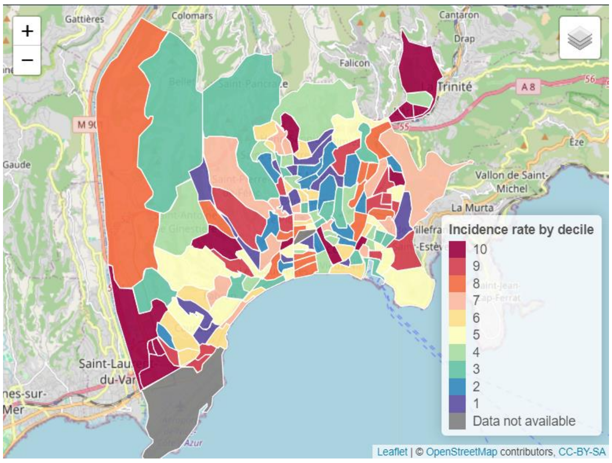

Figure 2 Spatial distribution of the cumulative incidence rate of COVID -19 by decile (from January 04 to February 14, 2021)

Figure 2 shows the spatial distribution of the COVID-19 incidence rate in the city of Nice. It can be seen that no part of Nice is spared. It can also be seen that the COVID-19 pandemic is concentrated in working-class neighborhoods in the extreme west and northeast of the city. This study period, which heralds the start of the third wave of the pandemic, shows the extent of the epidemiological situation in the city of Nice.

Table 1 OLS Regression

Variables	Model	T value	P value
Intercept	8.9710	3.647	0.000376***
LHDI	-4.8593	-1.958	0.052190 .
School (18-24)	-4.9436	-1.824	0.070373 .
Immigrant	4.1619	2.061	0.041172 *
Transport	-4.9433	-3.635	0.000392***
HLM rentals	2.0322	2.380	0.018667 *

OLS method was used to identify significant predictors of the prevalence of the COVID incidence rate in Nice. The selected OLS model explained 41.03% of the variation in the COVID incidence rate in Nice. The results of this model are presented in Table 1. We will keep these five variables to build future spatial models. The output of the OLS model shows that the proportion of immigrants and the proportion of the population living in low-income housing are positively correlated with the dependent variable, while the LHDI, the proportion of the working population using public transport and the proportion of young people aged 18 to 24 attending school are negatively correlated with the incidence rate of COVID-19.

Table 2 Global Moran's Index on the dependant variable

Indicator	Moran's I	Z-value	P-value
COVID incidence rate with first-order contiguity matrix	0,315	6,927	0,001
COVID incidence rate with 2nd-order contiguity matrix	0,031	1,0447	0,151
COVID incidence rate with distance weighted matrix	0,170	6,929	0,001

Spatial dependence was measured by defining a neighborhood structure for the 144 IRIS in the city of Nice. We begin by examining the results of the global Moran's I statistic (Table 2). A significantly positive Moran's I was obtained for both the first-order contiguity matrix and the distance-weighted matrix. The incidence rate of COVID-19 exhibited positive spatial autocorrelation suggesting a clustering pattern, with a statistically significant Moran's I value of 0.315 (p-value=0.001, z-value =5.64). These results indicate that the distribution of the incidence rate of COVID has a significant positive correlation with the incidence rate of the nearest neighborhoods during the study period in Nice.

Spatial autocorrelation of residuals allows us to check whether this dependency is captured by the model, or whether there are still unmodelled spatial structures (Table3). To do this, the Moran's I is calculated with the weight matrix used for the dependent variable on the residuals of the chosen classical linear regression. According to the table above, the Moran's I on the residuals are not statistically significant. This leads us to conclude that there is no significant spatial autocorrelation in the residuals of our model.

Table 3 Global Moran's Index on the residuals

Indicator	**Moran's I**	**Z-value**	**P-value**
Regression residuals with first-order contiguity matrix	-0,030	-0,4056	0,356
Regression residuals with 2nd-order contiguity matrix	-0,018	-0,3341	0,367
Regression residuals with distance weighted matrix	-0,051	-1,4627	0,053

Also, diagnostic tests, such as Lagrange multiplier tests, are required to assess the robustness of the model. The regression output allows us to diagnose the spatial dependence of the residuals using a number of tests (Appendix). Firstly, the Moran error test (-0 ,0508) with a very high p-value for the Moran's I residuals test (p = 0.13798), so we don't seem to have a global spatial relationship. The Lagrange multiplier test for the spatial lag model also has a fairly high p-value (p= 0.10633), and the insignificant Robust LM (lag) test suggests that a spatial lag model (SLM) may not be appropriate. This finding is reflected in the decision rule recommended by Anselin and Florax, which is based on the significance of the tests. Furthermore, the Lagrange Multiplier (error) (p-value=0.07964) and Robust LM (error) (p-value= 0.38707) tests mean that we cannot use the Spatial Error Model (SEM). Taken together, these tests show that there are no global dependencies. We can therefore conclude that there is local spatial dependence in our data.

The map bellow (figure3) represent the Local Indicator of Spatial Association in the city of Nice. It shows the formation of clusters of sick people during our study period. We find two statistically significant high-hight locations in the extreme western and extreme north-eastern parts of Nice in 8 IRIS. These zones indicate IRISs with high COVID-19 incidence rates, surrounded by other IRISs also characterized by high incidence rates. In Nice, this could represent neighborhoods or areas where the spread of the virus is particularly intense. A single statistically significant low-low location in the center of Nice in 35 IRIS. These areas correspond to IRISs with low COVID-19 incidence rates, surrounded by other IRISs also characterized by low incidence rates. This could represent neighborhoods where the spread of the virus is relatively under control, or where prevention measures are particularly effective. There are also other indicators that are not significant. There are 78 IRIS that are not significant, and 25 IRIS in the high-low and low-high categories that do not show the existence of clusters of people ill with

COVID-19. The city of Nice is thus characterized by an overall tendency towards spatial concentration of similar characteristics with strongly marked polarization patterns: we are faced with both forms of spatial autocorrelation (cluster formation) and spatial heterogeneity. Thus, positive local spatial dependence and the presence of clusters in the study area.

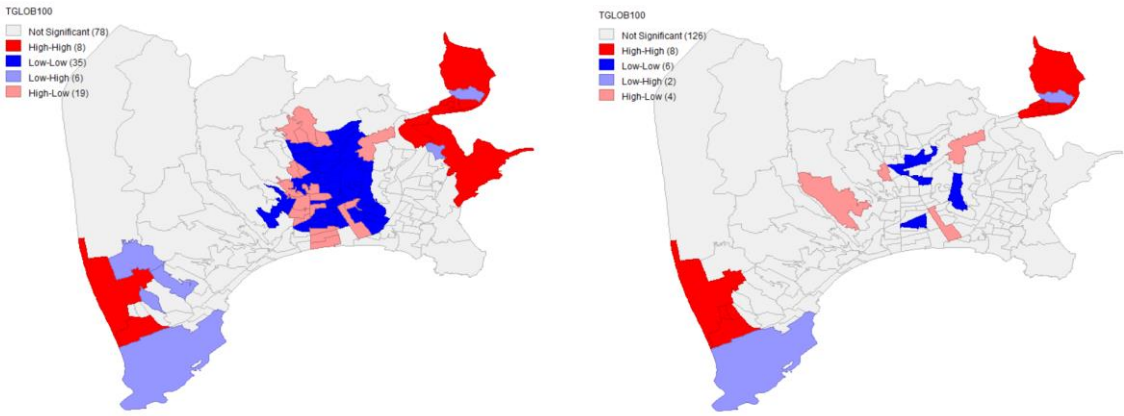

Figure 3 LISA distance / first-order QUEEN matrix on the COVID incidence rate.

Table 4 compares the bandwidths, effective number of parameters, critical t-values, R^2 and AICc for our two models. The statistical results presented in this show that the MGWR model is more relevant. The MGWR model explains 52% of the variance of the dependent variable

Table 4 Comparaison between GWR and MGWR

Diagnostics	GWR	MGWR						
	Model	Model	Intercept	IDHL	Personnes scol	Pop imm	Transports	HLM
Bandwidth	140		143	135	143	143	60	137
Degree of Dependency	0.889	0.827	0.939	0.887	0.938	0.920	0.630	0.857
Critical T (95 %)	2.209		2.105	2.212	2.109	2.145	2.687	2.271
AICc	342.074	337.163						
R^2	0.471	0.520						
N=144								

The MGWR summary results in table 5 also indicate that the MGWR model performs better than the GWR model, as the adjusted R^2 improves from 42% to 47% to explain the variation in the dependent variable and has a lower AIC (from 339.918 to 333.323).

Table 5 Summary of coefficients of dependants variables and descriptive statistics of model variables

Variables	GWR Model					MGWR Model				
	Err std	Min	Median	Max	Mean	Err std	Min	Median	Max	Mean
Intercept	0.041	-0.129	-0.013	0.050	-0.019 *	0.023	-0.142	-0.077	-0.041	-0.076 **
LDHI	0.028	-0.360	-0.286	-0.268	-0.299*	0.105	-0.460	-0.157	-0.127	-0.210 **
School (18-24)	0.022	-0.170	-0.120	-0.086	-0.123*	0.017	-0.150	-0.114	-0.083	-0.116 **
Immigrant	0.041	0.105	0.188	0.265	0.181*	0.021	0.184	0.213	0.265	0.217 **
Public transportation	0.032	-0.387	-0.317	-0.252	- 0.316***	0.165	-0.713	-0.222	-0.034	-0.280 ***
Social housing	0.134	0.026	0.152	0.513	0.201**	0.111	0.149	0.188	0.512	0.234 **
Quality of adjustement : R^2 adj = 0,429 (GWR) ; R^2 adj = 0,476(MGWR). AIC = 339,918 (GWR) ; AIC =333,323 (MGWR)										

Figures 4 to 8 map the spatial variation over the Nice city area of one unit added or decreased on the COVID incidence rate values provided by the socioeconomic variables. Maps in color blue shows the significant estimates of local parameters based on the significance of the p-value at the 5% threshold.

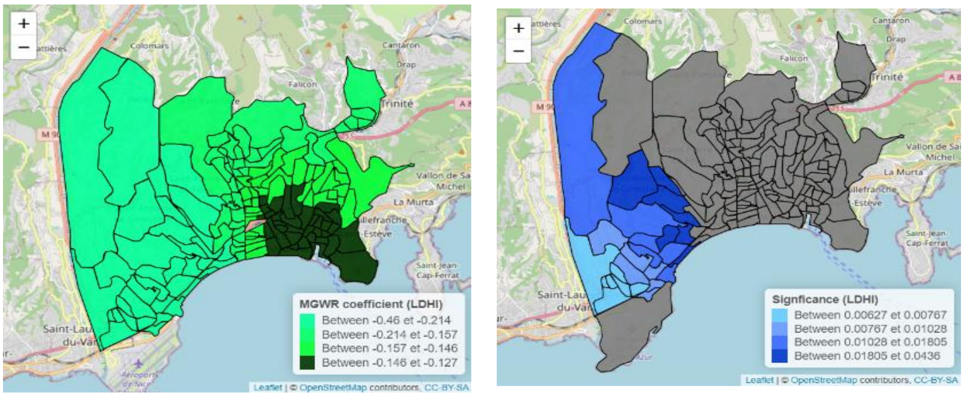

Figure 4 Coefficient and significance of the LHDI variable in the MGWR model

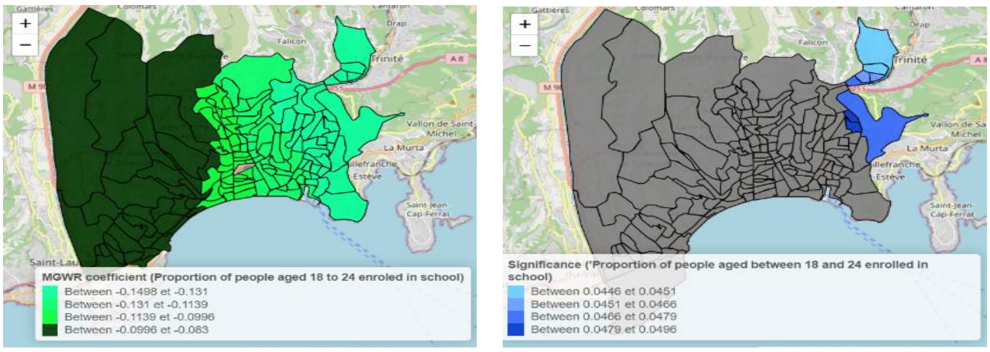

Figure 5 Coefficient and significance of the variable 'Proportion of people aged between 18 and 24 enrolled in school' in the MGWR model

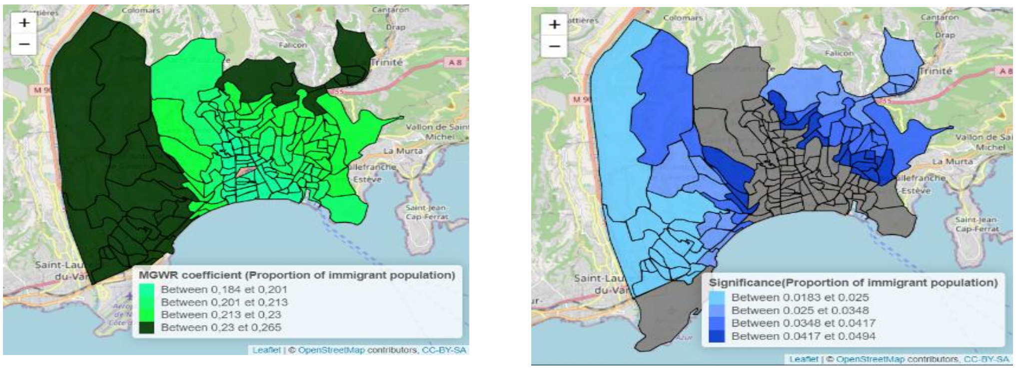

Figure 6 Coefficient and significance of the variable 'Proportion of immigrant population' in the MGWR model

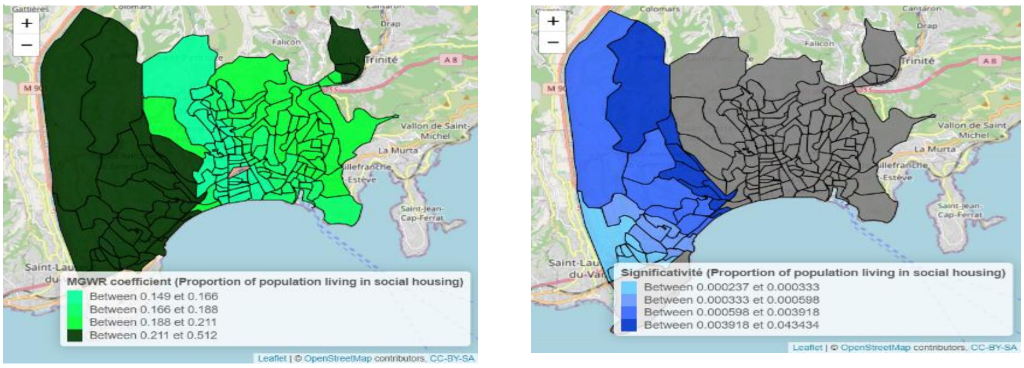

Figure 7 Coefficient and significance of the variable 'Proportion of population living in social housing'

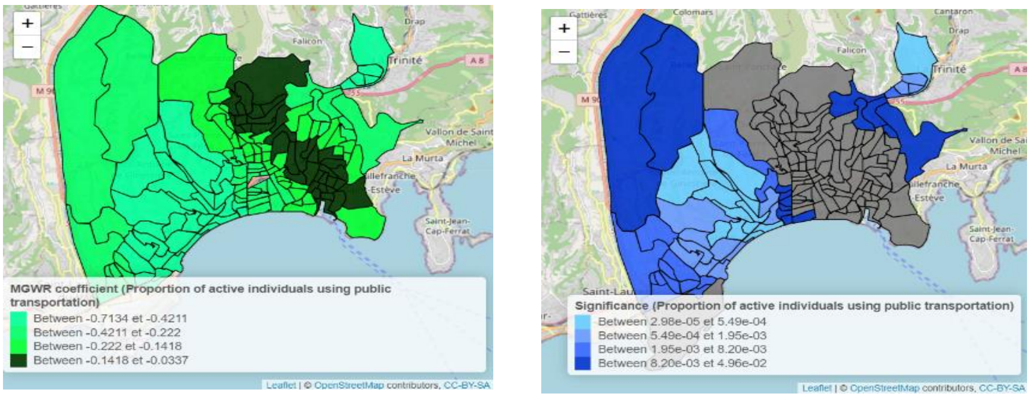

Figure 8 Coefficient and significance of the variable 'Proportion of active individuals using public transportation' in the MGWR model

The maps above show that all socio-economic factors have significant results. The LHDI, the proportion of 18-24 year olds in school and the proportion of working people using public transport all have a negative impact on the COVID-19 incidence rate. Evaluating the value of the incidence rate in relation to the LHDI, the overall model indicates that an increase of 0.1 in the LHDI is associated with a 31.9% decrease in the infection rate. This suggests that improving local human development conditions could have a significant impact on reducing infections. These single values are applied to the whole area. The spatial distribution shows that the highest estimates are observed to the south-east of the city of Nice, with a rate ranging from -0.146 to -0.127. The lowest estimates are in the extreme west of the city, with a rate ranging from -0.46 to -0.214 (Figure 4). Evaluating the value of the incidence rate in relation to the proportion of young people in school between the ages of 18 and 24, the global model estimates that the value of infected cases decreases by 12.3% for each unit increase in the proportion of young people in school. The spatial distribution shows that the highest estimates are observed to the west of the city of Nice, with rates ranging from -0.099 to -0.083. The lowest estimates are to the east of the city, with rates ranging from -0.149 to -0.131 (Figure 5). Evaluating the value of the incidence rate in relation to the proportion of working people using public transport, the overall model estimates that the value of infected cases decreases by 32.5% for every one-unit increase in the proportion of working people using public transport. The spatial distribution shows that the highest coefficients are observed in the city center, ranging from -0.141 to -0.034. (Figure 8).

As for the proportion of low-income housing and immigrants, these variables positively influence the COVID-19 incidence rate. The overall model estimates that the number of infected cases rises by 25.7% for every one-unit increase in the proportion of people living in low-income housing. The spatial distribution shows that the highest estimates are observed in the west, as well as in a few IRIS in the extreme east of the city, with coefficient variations ranging from 0.211 to 0.512. Neighborhoods where people living in low-income housing have a notable positive impact include areas such as Ariane and Pasteur (Figure 7). Finally, the overall model estimates that the value of infected cases increases by 21.8% for every one-unit increase in the immigrant proportion. These single values are applied to the zone as a whole. On the other hand, the figure shows that estimates of the immigrant proportion with the local model reveal a positive effect of an increase ranging from 0.23 to 0.265 in the extreme north-eastern and western parts of the city of Nice, while the lower ones reveal an increase ranging from 0.184 to 0.201 (Figure 6).

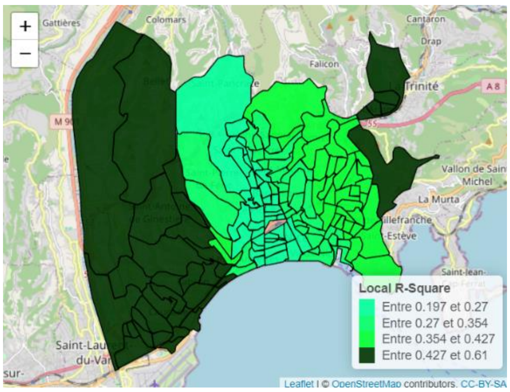

Figure 9 Local R-square

The R-squared (figure 9) value indicates that the MGWR model explains 52% of the variations in the COVID incidence rate in the city of Nice, which is higher than that of the OLS model. To illustrate this, figure 9 shows the spatial variations in local R^2 values in the study area of the COVID incidence rate associated with the MGWR model's socio-economic factors of COVID-19 disease distribution for each IRIS. The values with the highest R^2 ($0.427 \leq R^2 \leq 0.61$) are in the extreme eastern and western parts of the Nice commune. This indicates a strong prediction of concentration of infected cases in these areas. The values with the lowest R^2 are found in the center of Nice. This indicates the good performance of the MGWR model in this study area, since we find the same results as the clusters previously given by LISA.

IV- Discussion

Since the beginning of the twentieth century and throughout the history of pandemics, scientists have regarded human contact as a critical vector in the spatial spread of disease-causing viruses. Variations in this spread are often associated with socio-economic factors. In other words, different socio-economic groups may be vulnerable in different ways, depending on their lifestyles and social status.

In this analysis, we have highlighted five socio-economic factors to explain the spatial distribution of the incidence rate of COVID-19. A geographic information system (GIS) was used to visualize the geographical distribution of COVID-19 incidence in relation to these factors. A central question is whether the incidence rate of COVID-19 in one IRIS is influenced by that of neighboring IRIS's? In other words, is the spatial distribution of the incidence rate completely random? To answer this question, we compared two models: the local GWR model and the local MGWR model. The latter has been widely applied in a wide variety of scientific and socio-economic disciplines (GWR: Apparicio P et al. 2007[56]; Wheeler D. 2009[51]; Dziauddin MFet al. 2017[57]; Han Y et al. 2020[47]; Maiti et al. 2020[58] ; Shabrina Z et al. 2021[55]; Nushrat Nazia et al. 2022[30]; Lotfata A. 2022[59], MGWR: Maiti et al., 2020[58] ; Shabrina Z et al. 2021[55]; Nushrat Nazia et al. 2022[30]; Lotfata A. 2022[59] ; Ma et al. 2022[60]). For example Nushrat Nazia et al. have shown that there is heterogeneity between the distribution of COVID-infected cases and risk factors. They illustrated the spatial variation between the incidence rate of COVID and socio-economic factors using GWR.

The results show that the local MGWR model fits better, with an adjusted R^2= 0.476. The local Moran index, which measures spatial dependency, reveals the existence of three clusters in our study area: hot spots to the west and northeast of the city of Nice, and a cold spot in the center. The analysis revealed a significant negative association between the Localized Human Development Index (LHDI) and the incidence rate of COVID-19. This inverse relationship can be explained by the characteristics of this indicator, which assesses the standard of living in each area based not only on economic data, but also on the well-being of its inhabitants. The LHDI is a combination of three factors: life expectancy at birth, level of education and gross national income of each inhabitant. It ranges from 0 to 1, where 1 represents an improvement in well-being. This indicator captures the intrinsic vulnerability of populations, particularly those most affected by the virus[36]. Indeed, the coefficients of the MGWR model confirm this observation. We find that areas in working-class and disadvantaged neighborhoods have the highest incidence rates.

As shown in Figure 1, these areas are known for their concentration of social housing. Our model supports this finding, showing a significant positive association between the proportion of social housing and the proportion of immigrants and the incidence rate of COVID-19. The link between social housing and immigration is very strong. Figure 1 shows that the majority of immigrants live in low-income housing. This positive association can be explained by the more precarious living conditions (social housing, overcrowding) and working conditions (menial jobs) of this segment of the population, which may expose them more to the risk of contamination. Difficulties in accessing healthcare and information, notably due to language barriers[35] or socio-economic status[61] , are also contributing factors. Despite the various confinements and restrictions put in place, people of immigrant background faced an increased risk of exposure to the virus, reflecting social inequalities in health and ethno-racial discrimination. When collecting health data, patients' origins cannot legally be collected in France[31]. As mentioned above, this “virus of inequalities” has affected several types of people, particularly those most at risk from respiratory or chronic diseases. Immigrant and racialized communities were among the workers mobilized to help the population survive the crisis. Remotes work was not an option for them, given the types of jobs they held. In addition to their jobs, most of which were essential to the population's survival, other immigrants found themselves out of work due to the closure of businesses designated as non-essential, such as restaurants, hotels and domestic work. Professional vulnerability thus increased during the pandemic, particularly among immigrants. This not only increased the risk of contracting COVID, but also led to loss of income, deterioration in material conditions, financial stress and food insecurity. Thus, the high concentration of COVID among immigrants in Nice is due to socio-economic conditions, not physiological risks.

In our study, the proportion of young people aged between 18 and 24 attending school was not a factor in transmission, contrary to what might have been expected. One possible explanation is that our study period did not cover the entire duration of the pandemic; these IRIS might have been massively contaminated during the first waves of the epidemic and developed immunity by the time of our analysis.

As mentioned earlier, people using public transport to get to work were less likely to have COVID than those using their own vehicles. Despite the crowdedness of public transport, the spread of the virus was no greater, probably because the people using it respected the rules for wearing masks, although social distancing was impossible to apply. The risk of contamination with COVD is therefore lower if the barrier measures are respected. In addition, the daily disinfection of the transport network (buses, streetcars, subway trains and RERs), as well as stations, may have played a role in limiting the spread of the virus. Employment category is a concept that can interpret the LHDI variable as well as the transport variable. A person's occupational category may expose him or her to a major risk of contamination, and work may in most cases involve interaction with others, caused by frequent contact or the mode of transport used to get to the workplace[62]. Work that cannot be carried out at home, and therefore involves human contact, increases the risk of infection. Occupation is therefore a direct determinant of infection, as well as being an indirect determinant of the extent to which the disease spreads. Thus, work is correlated with level of education, a variable used to calculate the LHDI indicator. We can therefore conclude that a low level of education may be an indirect factor in the development of severe forms of COVID-19. A low level of education can also lead to low income, which can affect living conditions, such as housing in deprived areas, which can increase the risk of COVID and other pathogen infections.

Our study has a number of limitations, not least of which is the limited analysis period. A longer-term study would have enabled us to gain a better understanding of the dynamics of the spread of the COVID-19 epidemic in the city of Nice, and to identify more explanatory factors. In addition, our analysis was based on the cumulative incidence rate. Daily or weekly data might have been more appropriate for a finer spatial analysis.

V- Conclusion

The study period in this article was the most critical period in the spread of the COVID-19 virus in the city of NICE, with over 500 infected cases for every 100,000 people tested. Hence the interest in identifying and assimilating the elements that contributed to this deterioration. Geographical prediction can be useful in identifying various spatial distribution patterns and disease hotspots, and in detecting the most important risk factors. Such prediction is highly relevant to future interventions to combat disease transmissibility. Methodologically, this theoretical debate was empirically tested using the MGWR method as a local regression tool for COVID-19 disease traceability. The results show significant spatial heterogeneity in the local coefficients of the explanatory parameters of COVID-19 incidence. The illustration of the prediction of infected areas confirms that the most disadvantaged

IRIS in Nice are the most affected. But overall, we have seen that the city of Nice is in a very severe epidemiological situation. In our study, the well-being of individuals calculated by the LHDI, people living in low-income housing, the proportion of the population with a migrant background and the proportion of the population using public transport to get to work were the best predictors of variations in disease incidence rates. Geographical prevention of disease is very important, offering more informative results beyond the classic global model for rapid anticipatory development of IRIS-specific health policy.

1. Bellomo N, Bingham R, Chaplain MAJ, et al. A multiscale model of virus pandemic: Heterogeneous interactive entities in a globally connected world. *Math Models Methods Appl Sci*. 2020;30(08):1591-1651. doi:10.1142/S0218202520500323

2. The Challenges and Opportunities in Creating an Early Warning System for Global Pandemics. Accessed January 27, 2025. https://www.researchgate.net/publication/368159495_The_Challenges_and_Opportunities_in_Creating_an_Early_Warning_System_for_Global_Pandemics

3. À la lumière de la pandémie. Une nouvelle stratégie en faveur de la santé et du développement durable. Accessed January 27, 2025. https://www.who.int/europe/fr/publications/m/item/drawing-light-from-the-pandemic--a-new-strategy-for-health-and-sustainable-development

4. Schellekens P, Sourrouille D. *COVID-19 Mortality in Rich and Poor Countries: A Tale of Two Pandemics?* World Bank, Washington, DC; 2020. doi:10.1596/1813-9450-9260

5. Shahbazi F, Khazaei S. Socio-economic inequality in global incidence and mortality rates from coronavirus disease 2019: an ecological study. *New Microbes New Infect*. 2020;38:100762. doi:10.1016/j.nmni.2020.100762

6. Revollo-Fernández D, Rodríguez-Tapia L, Medina-Rivas C, Morales-Novelo JA. Socio-economic determinants of COVID-19 in Mexico. *Public Health*. 2022;207:28-30. doi:10.1016/j.puhe.2022.03.011

7. Etowa J, Hyman I. Unpacking the health and social consequences of COVID-19 through a race, migration and gender lens. *Can J Public Health*. 2021;112(1):8-11. doi:10.17269/s41997-020-00456-6

8. Ruthberg J, Quereshy H, Jella T, et al. Geospatial analysis of COVID-19 and otolaryngologists above age 60. *American Journal of Otolaryngology*. 2020;41:102514. doi:10.1016/j.amjoto.2020.102514

9. Xu XW, Wu XX, Jiang XG, et al. Clinical findings in a group of patients infected with the 2019 novel coronavirus (SARS-Cov-2) outside of Wuhan, China: retrospective case series. *BMJ*. 2020;368:m606. doi:10.1136/bmj.m606

10. Luo Y, Yan J, McClure S. Distribution of the environmental and socioeconomic risk factors on COVID-19 death rate across continental USA: a spatial nonlinear analysis. *Environ Sci Pollut Res Int*. 2021;28(6):6587-6599. doi:10.1007/s11356-020-10962-2

11. Patterson K, Chalifoux M, Gad R, et al. Tendances démographiques de l’exposition à une éclosion de COVID-19 et de la transmission de cas dans une communauté rurale canadienne, 2020. *RMTC*. 2022;48(10):512-519. doi:10.14745/ccdr.v48i10a06f

12. Dowrick A, Rai T, Hinton L, et al. Health inequalities, ethnic minorities and COVID19: interactive theatre workshop drawing on a qualitative interview study. *Lancet*. 2022;400 Suppl 1:S9. doi:10.1016/S0140-6736(22)02219-X

13. Godefroy R, Lewis J. What explains the socioeconomic status-health gradient? Evidence from workplace COVID-19 infections. *SSM Popul Health*. 2022;18:101124. doi:10.1016/j.ssmph.2022.101124

14. Benita F, Rebollar-Ruelas L, Gaytán-Alfaro ED. What have we learned about socioeconomic inequalities in the spread of COVID-19? A systematic review. *Sustain Cities Soc*. 2022;86:104158. doi:10.1016/j.scs.2022.104158

15. Etowa J, Hyman I, Dabone C, et al. Strengthening the Collection and Use of Disaggregated Data to Understand and Monitor the Risk and Burden of COVID-19 Among Racialized Populations. *Can Stud Popul*. 2021;48(2-3):201-216. doi:10.1007/s42650-021-00050-2

16. Bambra C, Riordan R, Ford J, Matthews F. The COVID-19 pandemic and health inequalities. *J Epidemiol Community Health*. 2020;74(11):964-968. doi:10.1136/jech-2020-214401

17. Rohleder S, Costa DD, Bozorgmehr PK. Area-level socioeconomic deprivation, non-national residency, and Covid-19 incidence: A longitudinal spatiotemporal analysis in Germany. *eClinicalMedicine*. 2022;49. doi:10.1016/j.eclinm.2022.101485

18. Chossegros P. L'épidémie de COVID-19 : une autre histoire pourrait être racontée. *La Presse Médicale Formation*. 2020;1(5):447-450. doi:10.1016/j.lpmfor.2020.09.012

19. Patel JA, Nielsen FBH, Badiani AA, et al. Poverty, inequality and COVID-19: the forgotten vulnerable. *Public Health*. 2020;183:110-111. doi:10.1016/j.puhe.2020.05.006

20. Fontán-Vela M, Gullón P, Bilal U, Franco M. Social and ideological determinants of COVID-19 vaccination status in Spain. *Public Health*. 2023;219:139-145. doi:10.1016/j.puhe.2023.04.007

21. Siljander M, Uusitalo R, Pellikka P, Isosomppi S, Vapalahti O. Spatiotemporal clustering patterns and sociodemographic determinants of COVID-19 (SARS-CoV-2) infections in Helsinki, Finland. *Spatial and Spatio-temporal Epidemiology*. 2022;41:100493. doi:10.1016/j.sste.2022.100493

22. Talavera A, Perez EM. Is cholera disease associated with poverty? *The Journal of Infection in Developing Countries*. 2009;3(06):408-411. doi:10.3855/jidc.410

23. Scott A, Coote W. Incentives and the Quality of Primary Care in Australia: Do Regional Primary Care Organisations Make a Difference? Published online June 19, 2007. Accessed August 24, 2023. https://papers.ssrn.com/abstract=995067

24. Hu Y, Goldman N. Mortality Differentials by Marital Status: An International Comparison. *Demography*. 1990;27(2):233-250. doi:10.2307/2061451

25. Frohlich N, Mustard C. A regional comparison of socioeconomic and health indices in a Canadian province. *Social Science & Medicine*. 1996;42(9):1273-1281. doi:10.1016/0277-9536(95)00220-0

26. Recensement 2019 : résultats sur un territoire, bases de données et fichiers détail | Insee. Accessed August 26, 2024. https://www.insee.fr/fr/information/6444222

27. Dossier complet − Commune de Nice (06088) | Insee. Accessed November 14, 2023. https://www.insee.fr/fr/statistiques/2011101?geo=COM-06088#chiffre-cle-5

28. travail M du, solidarités de la santé et des, travail M du, solidarités de la santé et des. Professionnels de santé. Ministère du travail, de la santé et des solidarités. March 18, 2024. Accessed March 18, 2024. https://sante.gouv.fr/soins-et-maladies/maladies/maladies-infectieuses/coronavirus/professionnels-de-sante/

29. Système de surveillance du COVID-19 : pour une analyse territoriale contextualisée de la dynamique épidémique. Accessed August 24, 2023. https://www.santepubliquefrance.fr/presse/2020/systeme-de-surveillance-du-covid-19-pour-une-analyse-territoriale-contextualisee-de-la-dynamique-epidemique

30. Nazia N, Law J, Butt ZA. Spatiotemporal clusters and the socioeconomic determinants of COVID-19 in Toronto neighbourhoods, Canada. *Spatial and Spatio-temporal Epidemiology*. 2022;43:100534. doi:10.1016/j.sste.2022.100534

31. Brun S, Simon P. L'invisibilité des minorités dans les chiffres du Coronavirus : le détour par la Seine-Saint-Denis. *De Facto - Institut Convergences Migrations*. 2020;(19):68-78.

32. Pinter-Wollman N, Jelić A, Wells NM. The impact of the built environment on health behaviours and disease transmission in social systems. *Philos Trans R Soc Lond B Biol Sci*. 2018;373(1753):20170245. doi:10.1098/rstb.2017.0245

33. Cordes J, Castro MC. Spatial analysis of COVID-19 clusters and contextual factors in New York City. *Spatial and Spatio-temporal Epidemiology*. 2020;34:100355. doi:10.1016/j.sste.2020.100355

34. Vilinová K, Petrikovičová L. Spatial Autocorrelation of COVID-19 in Slovakia. *Tropical Medicine and Infectious Disease*. 2023;8(6):298. doi:10.3390/tropicalmed8060298

35. Vang ZM, Ng E. The impacts of COVID-19 on immigrants and the healthy immigrant effect: Reflections from Canada. *Preventive Medicine*. 2023;171:107501. doi:10.1016/j.ypmed.2023.107501

36. Scarpone C, Brinkmann ST, Große T, Sonnenwald D, Fuchs M, Walker BB. A multimethod approach for county-scale geospatial analysis of emerging infectious diseases: a cross-sectional case study of COVID-19 incidence in Germany. *International Journal of Health Geographics*. 2020;19(1):32. doi:10.1186/s12942-020-00225-1

37. Kim S, Castro MC. Spatiotemporal pattern of COVID-19 and government response in South Korea (as of May 31, 2020). *International Journal of Infectious Diseases*. 2020;98:328-333. doi:10.1016/j.ijid.2020.07.004

38. Le Gallo J. Économétrie spatiale : l'autocorrélation spatiale dans les modèles de régression linéaire. *Économie & prévision*. 2002;155(4):139-157. doi:10.3917/ecop.155.0139

39. MORAN PAP. NOTES ON CONTINUOUS STOCHASTIC PHENOMENA. *Biometrika*. 1950;37(1-2):17-23. doi:10.1093/biomet/37.1-2.17

40. Oliveau S. Autocorrélation spatiale : leçons du changement d'échelle. *L'Espace géographique*. 2010;39(1):51-64. doi:10.3917/eg.391.0051

41. Cliff A, Ord K. Testing for Spatial Autocorrelation Among Regression Residuals. *Geographical Analysis*. 1972;4(3):267-284. doi:10.1111/j.1538-4632.1972.tb00475.x

42. Gaspard G, Kim D, Chun Y. Residual spatial autocorrelation in macroecological and biogeographical modeling: a review. *Journal of Ecology and Environment*. 2019;43(1):19. doi:10.1186/s41610-019-0118-3

43. Guillain R, Le Gallo J. Identifier la localisation des activités économiques : une approche par les outils de l'analyse exploratoire des données spatiales. *Économie appliquée*. 2008;61(3):5-34. doi:10.3406/ecoap.2008.1883

44. Oliveau S. Les indicateurs locaux d'association spatiale (LISA) comme méthode de régionalisation: Une application en Inde. Published online 2005.

45. Anselin L, Rey S. Properties of Tests for Spatial Dependence in Linear Regression Models. *Geographical Analysis*. 1991;23(2):112-131. doi:10.1111/j.1538-4632.1991.tb00228.x

46. Fotheringham A, Brunsdon C, Charlton M. Geographically Weighted Regression: The Analysis of Spatially Varying Relationships. *John Wiley & Sons*. 2002;13.

47. Han Y, Yang L, Jia K, et al. Spatial distribution characteristics of the COVID-19 pandemic in Beijing and its relationship with environmental factors. *Science of The Total Environment*. 2021;761:144257. doi:10.1016/j.scitotenv.2020.144257

48. Lu B, Brunsdon C, Charlton M, Harris P. Geographically weighted regression with parameter-specific distance metrics. *International Journal of Geographical Information Science*. 2017;31(5):982-998. doi:10.1080/13658816.2016.1263731

49. Fotheringham AS, Brunsdon C, Charlton M. *Geographically Weighted Regression: The Analysis of Spatially Varying Relationships*. John Wiley & Sons; 2003.

50. Brunsdont C, Fotheringham S, Charlton M. Geographically weighted regression - Modelling spatial non-stationarity. *Journal of the Royal Statistical Society Series D: The Statistician*. 1998;47(3):431-443. doi:10.1111/1467-9884.00145

51. Wheeler D. Simultaneous Coefficient Penalization and Model Selection in Geographically Weighted Regression: The Geographically Weighted Lasso. *Environment and Planning A*. 2009;41:722-742. doi:10.1068/a40256

52. Fotheringham AS, Yang W, Kang W. Multiscale Geographically Weighted Regression (MGWR). *Annals of the American Association of Geographers*. 2017;107(6):1247-1265. doi:10.1080/24694452.2017.1352480

53. Yu H, Fotheringham AS, Li Z, Oshan T, Wolf LJ. On the measurement of bias in geographically weighted regression models. *Spatial Statistics*. 2020;38:100453. doi:10.1016/j.spasta.2020.100453

54. Oshan TM, Li Z, Kang W, Wolf LJ, Stewart Fotheringham A. MGWR: A python implementation of multiscale geographically weighted regression for investigating process spatial heterogeneity and scale. *ISPRS International Journal of Geo-Information*. 2019;8(6). doi:10.3390/ijgi8060269

55. Shabrina Z, Buyuklieva B, Ng MKM. Short-Term Rental Platform in the Urban Tourism Context: A Geographically Weighted Regression (GWR) and a Multiscale GWR (MGWR) Approaches. *Geographical Analysis*. 2021;53(4):686-707. doi:10.1111/gean.12259

56. Apparicio P, Séguin AM, Leloup X. Modélisation spatiale de la pauvretéà Montréal: apport méthodologique de la régression géographiquement pondérée. *Canadian Geographies / Géographies canadiennes*. 2007;51(4):412-427. doi:10.1111/j.1541-0064.2007.00189.x

57. Dziauddin MF, Idris Z. Use of Geographically Weighted Regression (GWR) Method to Estimate the Effects of Location Attributes on the Residential Property Values. *Indonesian Journal of Geography*. 2017;49(1):97-110. doi:10.22146/ijg.27036

58. Maiti A, Zhang Q, Sannigrahi S, Pramanik S, Chakraborti S, Pilla F. Spatiotemporal effects of the causal factors on COVID-19 incidences in the contiguous United States. *Sustainable Cities and Society*. 2021;68:102784. doi:10.1016/j.scs.2021.102784

59. Lotfata A. Using Geographically Weighted Models to Explore Obesity Prevalence Association with Air Temperature, Socioeconomic Factors, and Unhealthy Behavior in the USA. *J geovis spat anal*. 2022;6(1):14. doi:10.1007/s41651-022-00108-y

60. Ma J, Zhu H, Li P, et al. Spatial Patterns of the Spread of COVID-19 in Singapore and the Influencing Factors. *ISPRS International Journal of Geo-Information*. 2022;11(3):152. doi:10.3390/ijgi11030152

61. Kirksey L, Tucker DL, Taylor E, White Solaru KT, Modlin CS. Pandemic Superimposed on Epidemic: Covid-19 Disparities in Black Americans. *Journal of the National Medical Association*. 2021;113(1):39-42. doi:10.1016/j.jnma.2020.07.003

62. Rule AM, Apau O, Ahrenholz SH, et al. Healthcare personnel exposure in an emergency department during influenza season. *PLoS One*. 2018;13(8):e0203223. doi:10.1371/journal.pone.0203223

Appendix:

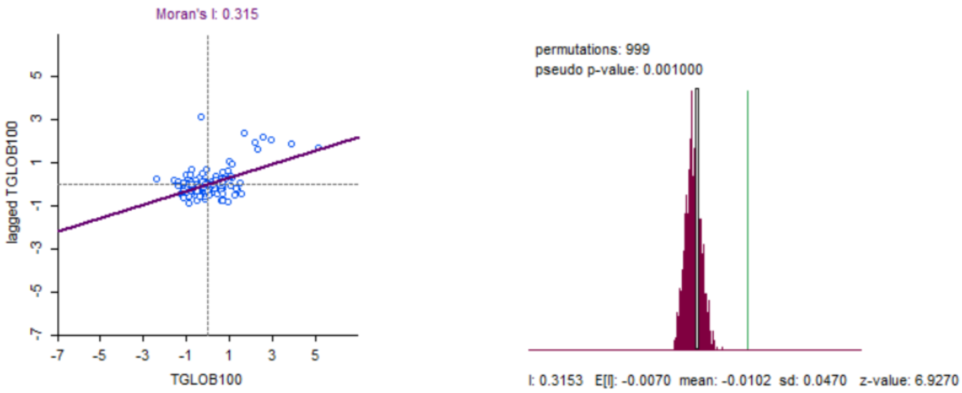

first-order contiguity matrix

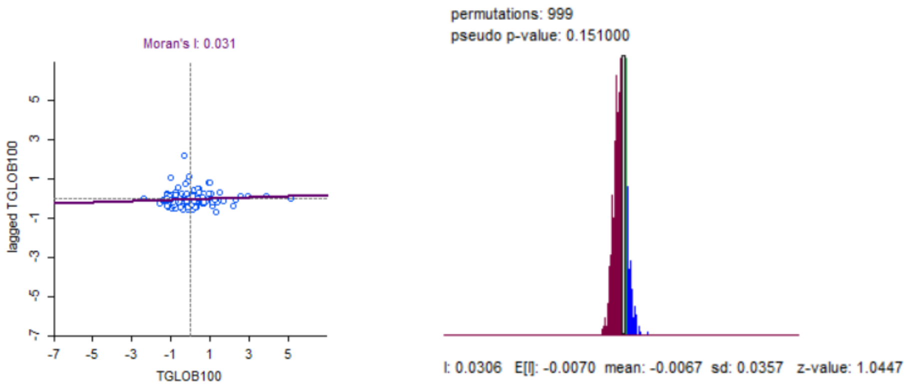

2nd order contiguity matrix

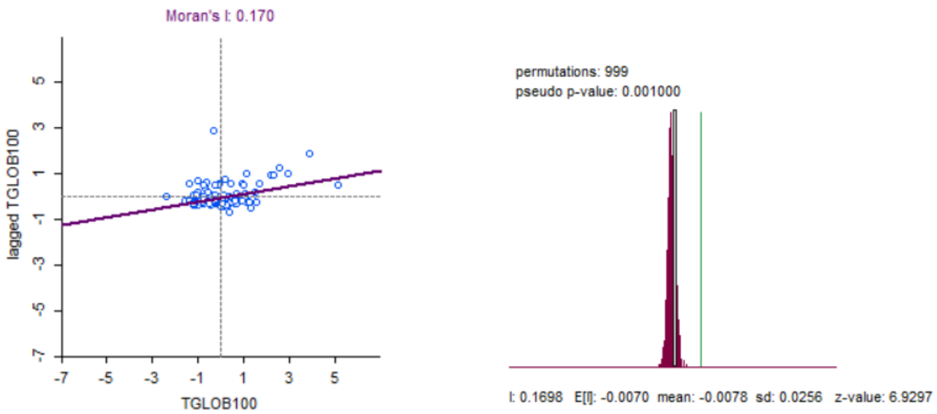

Distance matrix

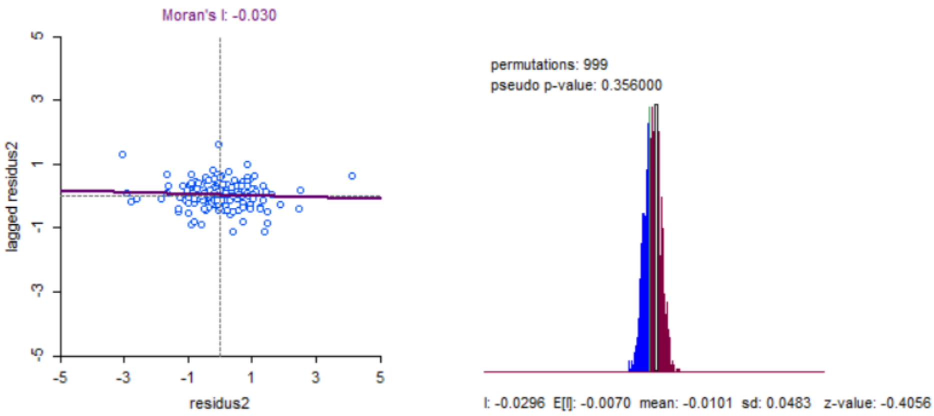

Moran residuals with first-order contiguity matrix

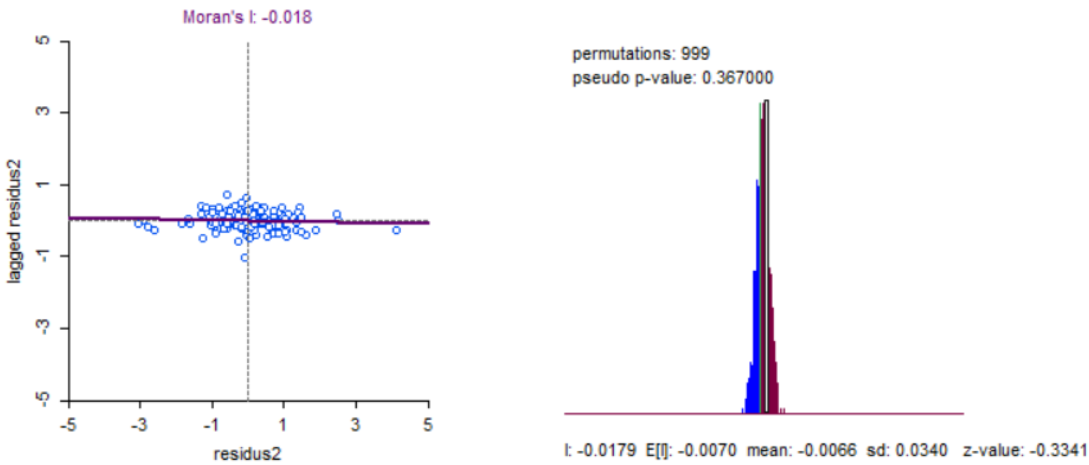

Moran residuals with 2nd-order contiguity matrix

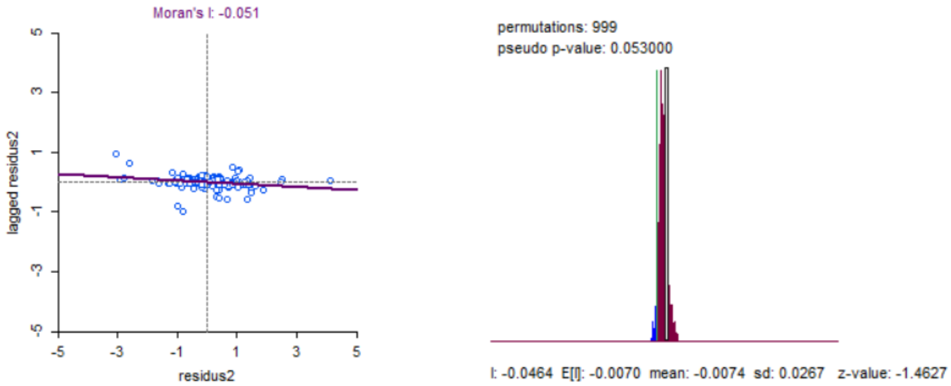

Moran residuals with distance matrix

DIAGNOSTICS FOR SPATIAL DEPENDENCE
FOR WEIGHT MATRIX : NIZZA_3
(row-standardized weights)

TEST	MI/DF	VALUE	PROB
Moran's I (error)	-0.0296	-0.1332	0.89405
Lagrange Multiplier (lag)	1	0.0084	0.92691
Robust LM (lag)	1	1.7515	0.18569
Lagrange Multiplier (error)	1	0.3486	0.55492
Robust LM (error)	1	2.0916	0.14811
Lagrange Multiplier (SARMA)	2	2.1000	0.34993

============================== END OF REPORT ================================

Regression with geoda, weight matrix: first-order contiguity

DIAGNOSTICS FOR SPATIAL DEPENDENCE
FOR WEIGHT MATRIX : NIZZA_3D
(row-standardized weights)

TEST	MI/DF	VALUE	PROB
Moran's I (error)	-0.0508	-1.4833	0.13798
Lagrange Multiplier (lag)	1	2.6080	0.10633
Robust LM (lag)	1	0.2838	0.59424
Lagrange Multiplier (error)	1	3.0723	0.07964
Robust LM (error)	1	0.7481	0.38707
Lagrange Multiplier (SARMA)	2	3.3561	0.18674

============================== END OF REPORT ================================

Regression with geoda, weight matrix: Distance

DOCUMENTS DE TRAVAIL GREDEG PARUS EN 2025
GREDEG Working Papers Released in 2025